Author Manuscript

Author Manuscript

Author Manuscript

Author Manuscript

HHS Public Access

Author manuscript

*Nat Microbiol*. Author manuscript; available in PMC 2018 November 01.

Published in final edited form as:

*Nat Microbiol*. 2017 November ; 2(11): 1480–1484. doi:10.1038/s41564-017-0023-4.

# A viral protein antibiotic inhibits lipid II flippase activity

**Karthik R. Chamakura**[1], **Lok-To Sham**[2], **Rebecca M. Davis**[3], **Lorna Min**[1], **Hongbaek Cho**[2], **Natividad Ruiz**[3], **Thomas G. Bernhardt**[2,*], and **Ry Young**[1,*]

[1]Center for Phage Technology, Department of Biochemistry and Biophysics, Texas A&M AgriLife Research, Texas A&M University, College Station, TX 77843-2128, USA

[2]Department of Microbiology and Immunobiology, Harvard Medical School, Boston, MA 02215, USA

[3]Department of Microbiology, Ohio State University, Columbus, OH 43210, USA

## Abstract

For bacteriophage infections, the cell walls of bacteria, consisting of a single highly polymeric molecule of peptidoglycan (PG), pose a major problem for the release of progeny virions. Phage lysis proteins that overcome this barrier can point the way to new antibacterial strategies[1], especially small lytic single-stranded DNA (the microviruses) and RNA phages (the leviviruses) that effect host lysis using a single non-enzymatic protein[2]. Previously, the $A_2$ protein of levivirus Qβ and the E protein of the microvirus φ X174 were shown to be 'protein antibiotics' that inhibit the MurA and MraY steps of the PG synthesis pathway[2–4]. Here, we investigated the mechanism of action of an unrelated lysis protein, $Lys^M$, of the *Escherichia coli* levivirus M[5]. We show that $Lys^M$ inhibits the translocation of the final lipid-linked PG precursor called lipid II across the cytoplasmic membrane by interfering with the activity of MurJ. The finding that $Lys^M$ inhibits a distinct step in the PG synthesis pathway from the $A_2$ and E proteins indicates that small phages, particularly the single-stranded RNA (ssRNA) leviviruses, have a previously unappreciated capacity for evolving novel inhibitors of PG biogenesis despite their limited coding potential.

Recently, Rumnieks and Tars (2012) surveyed the few available ssRNA phage genomes (Fig. 1a) and found that lysis genes appear to have evolved at different sites after speciation of the phage to infect cells with new pili receptors[5]. In particular, levivirus M has its $lys^M$ gene embedded in the +1 reading frame of *rep*. We observed that expression of $lys^M$ from a multi-copy plasmid induced morphological defects prior to lysis that were similar to those caused

**Reprints and permissions information** is available at www.nature.com/reprints.

*Correspondence and requests for materials should be addressed to T.G.B. or R.Y. thomas@hms.harvard.edu; ryland@tamu.edu.

**Author contributions**

K.R.C., N.R., T.G.B. and R.Y. designed the study and the analysed results. K.R.C. performed genetic selections and microscopy, and constructed strains and plasmids. L.-T.S. performed ColM assays and performed the *amJ* rescue experiment. R.M.D. constructed various *murJ* haploid strains, performed their function and expression tests, and performed SCAM. L.M. performed lysis profiles of the $Lys^M$-resistant alleles and assisted in making the figures. H.C. constructed the *E. coli* multi-copy library. K.R.C., T.G.B. and R.Y. prepared the manuscript. N.R. and L.-T.S. edited the manuscript and provided text.

**Competing interests**

The authors declare no competing financial interests.

Supplementary information is available for this paper at doi:10.1038/s41564-017-0023-4.

Author Manuscript Author Manuscript Author Manuscript Author Manuscript

by $A_2$, E and beta-lactams, suggesting that $Lys^M$ might also inhibit PG biosynthesis (Fig. 1b,c and Supplementary Fig. 1). To identify its target, we introduced a multi-copy plasmid library containing random fragments of the *E. coli* genome to cells producing $Lys^M$ and selected for lysis-resistant clones. Three of the survivors contained plasmids carrying *murJ* (Supplementary Fig. 2 and Supplementary Table 1), indicating that elevated MurJ production protects cells from $Lys^M$, which normally accumulates to about five times the level of MurJ at the time of lysis (Supplementary Fig. 3). Further support for MurJ being the $Lys^M$ target came from the isolation of spontaneous mutants in *murJ* promoting resistance to *lys*$^M$ expression (Fig. 1d and Supplementary Fig. 4a,b).

MurJ and another protein, FtsW, have both been proposed to be the lipid II flippase of the PG synthesis pathway that translocates the final PG precursor across the cytoplasmic membrane[6–8]. Evidence for FtsW having this activity is based on an in vitro proteoliposome assay[8]. However, FtsW has not been found to be critical for lipid II translocation in vivo[6]. MurJ, on the other hand, has been shown to be essential for PG synthesis and lipid II flipping in vivo[6,7]. Moreover, it is related to transporters implicated in translocating other lipid-linked polysaccharide precursors such as those for O-antigen synthesis[9]. Finally, chemical probing and a recently published crystal structure indicate that MurJ has a solvent-exposed cavity consistent with it functioning as a transporter[10,11.]

Amino-acid substitutions in MurJ resulting in $Lys^M$-resistance cluster in two of its fourteen transmembrane domains (TMDs), TMD2 and TMD7, which form part of the solvent-exposed cavity (Fig. 2 and Supplementary Table 2). None of these changes affected MurJ accumulation (Supplementary Fig. 5). We used thiol accessibility (substituted-cysteine accessibility method (SCAM)) to address whether $Lys^M$ affected MurJ conformation in the membrane. Cysteine substitutions in ten positions in MurJ were tested for reactivity to the thiol reagents MTSES (sodium (2-sulfonato-ethyl) methanethiosulfonate; membrane-impermeable) and NEM (*N*-ethylmaleimide; membrane-permeable) in cells producing $Lys^M$–cmyc (Fig. 3 and Supplementary Fig. 6). The SCAM reactivity patterns for five positions in aqueous domains were unaffected by *lys*$^M$ induction, but five TMD positions exhibited altered MTSES sensitivity, with four being converted from partial to complete reactivity. These results suggest that $Lys^M$ binds to MurJ and causes a conformational change that locks MurJ into one of the two conformations proposed to constitute the lipid II flipping cycle, with the solvent-filled cavity facing either the periplasm or cytoplasm[10–12] (Supplementary Fig. 7). Accordingly, induction of *lys*$^M$ in cells overexpressing non-functional alleles of *murJ* that produce normal levels of protein[12] did not protect against $Lys^M$-dependent lysis, whereas the wild-type allele does (Supplementary Fig. 4d).

To assess the effect of $Lys^M$ on MurJ-dependent lipid II flipping activity, we used a previously published in vivo flippase assay[6,13]. In this assay, cells are radiolabelled with the PG precursor [$^3$H]mesodiaminopimelic acid (mDAP) and treated with colicin M (ColM), a toxin that invades the periplasm to cleave flipped lipid II, generating a soluble pyrophospho-disaccharide pentapeptide that is subsequently converted to disaccharide tetrapeptide by periplasmic carboxypeptidases. The other product is undecaprenol, a probably dead-end derivative of the lipid carrier that cannot be reused[6,14]. Thus, ColM function blocks PG synthesis (Supplementary Fig. 9), irreversibly removes radiolabel from the PG lipid

Author Manuscript Author Manuscript Author Manuscript Author Manuscript

precursor pool, and leads to the production of a new soluble radiolabelled product. Inactivation of MurJ function was previously shown to prevent lipid II cleavage by ColM by blocking lipid II translocation across the membrane, thus leading to the protection of the radiolabelled PG lipid precursor pool and the absence of the ColM soluble product[6]. $Lys^M$ production similarly blocked depletion of the PG lipid precursor pool by ColM (Fig. 4a and Supplementary Fig. 10). However, in cells producing a $Lys^M$-resistant variant of MurJ, $MurJ^{M233L, I248S}$ (Supplementary Fig. 4c), $Lys^M$ production was unable to prevent lipid II cleavage by ColM, indicating that flipping remained active. Finally, in addition to alterations in MurJ, overproduction of the unrelated (alternative) lipid II flippase Amj from *Bacillus subtilis*[13] also promoted resistance to $Lys^M$ production (Supplementary Fig. 11). We therefore conclude that the phage M lysis gene is likely to encode a specific inhibitor of MurJ that blocks lipid II flipping. Although direct binding of $Lys^M$ to MurJ remains to be demonstrated, $Lys^M$ clearly joins the E and $A_2$ proteins as the third instance of a 'protein antibiotic' targeting an essential step of PG biosynthesis.

The φ X174 E protein inhibits MraY[15] and is encoded in the +1 reading frame of an essential morphogenesis gene (Fig. 1a). Maturation proteins are present as a single molecule on the capsid of all leviviruses[16], serving to recognize and bind to the F pilus. However, in Qβ, the maturation protein $A_2$ has evolved an additional ability to inhibit MurA[4]. Like these factors, *lys*$^M$ occupies no dedicated genetic space[5], highlighting the ability of small phages to maximize their coding capacity. Recent analysis of publicly available metagenomes and transcriptomes has revealed that the ssRNA leviviruses are more ubiquitous and diverse than previously appreciated[17,18], at least in part because of extensive use of RNase during virome sampling. RNA phages are therefore estimated to constitute a substantial fraction of the total virome in gut samples[19], representing a deep resource of genomic 'dark matter'. Our results suggest that leviviruses, empowered by the error-prone character of their RNA replicase[20,21] and economic use of genomic space, are capable of generating a vast environmental library of small proteins that can block a variety of steps in PG synthesis. The genetics of ssRNA phages may thus turn out to be powerful tools for identifying targetable sites in cell wall biogenesis enzymes to aid the development of new antibiotics.

## Methods

### Bacterial strains, plasmids and growth conditions

The bacterial strains and plasmids used in this study are listed in Supplementary Table 3. Primers are listed in Supplementary Table 4. Cultures were grown with aeration at 37 °C in lysogeny broth (LB) supplemented with ampicillin (100 μg $ml^{-1}$), chloramphenicol (10 or 25 μg $ml^{-1}$) and L-arabinose (0.4% w/v), when indicated isopropyl-β-D-thiogalactopyranoside (IPTG; RPI) at 25 μM or 50 μM final concentration was added, and 20 μg $ml^{-1}$ final 5-bromo-4-chloro-indolyl-β-D-galactopyranoside (X-Gal) when indicated. All chemicals were supplied by Sigma Aldrich unless otherwise indicated. The Δ*pyrC::kan* allele was obtained from Keio collection[22] and was transduced into appropriate strains by P1 transduction[23].

Plasmid pKC3 (*bla araC* $P_{ara}$*::lys–his*$_6$ *lacZα*) encoding a hexahistidine-tagged $Lys^M$ was constructed in multiple steps. First, a synthetic construct was obtained (GenScript)

Author Manuscript Author Manuscript Author Manuscript Author Manuscript

containing the DNA sequence from phage M (accession number: JX625144) encompassing the *lys* gene and *lacZα*, flanked by restriction sites for EcoRI and XhoI/HindIII upstream and downstream, respectively, to facilitate cloning, and with its start codon changed from TTG to ATG. This *lys* construct was sub-cloned into pBAD24 between the EcoRI and HindIII sites to yield pKC1. Codons encoding a hexa-histidine tag were inserted at the 3′ end of *lys* in pKC1 through site-directed mutagenesis with the primer KC163, to generate pKC2. The resulting *lys–his6* gene was amplified from pKC2 by PCR with primers KC30 and KC210 and Pfu DNA polymerase. The PCR product was digested with EcoRI and XhoI and cloned between the corresponding sites in pKC1 to yield pKC3. The cloned fragments at each step were verified by sequencing.

A *lys* gene modified at its 3′ end with codons for the cmyc tag (GEQKLISEEDLNSAVD) was obtained as part of a gBlock (IDT) containing flanking KpnI and HindIII sites. Plasmid pKC4 (*bla araC* $p_{ara}$*::lys-cmyc)* was constructed by digesting the gBlock with KpnI and HindIII and ligating the product into the corresponding sites in the vector pBAD30.

The plasmid pKC5 (*cat araC* $p_{ara}$*::lys-cmyc*) was constructed by sub-cloning *lys–cmyc* from pKC4 to pBAD33 with KpnI and HindIII.

The plasmid pKC6 (*bla araC* $p_{ara}$*::lysC10S–cmyc)* was constructed in a similar way to pKC4 where the codon for cysteine at position 10 was changed to serine.

The plasmid pKC7 (*bla araC* $p_{ara}$*::lys–eGFP*) was constructed by cloning of *lys–eGFP* gBlock into pBAD30 vector digested with KpnI and HindIII.

The plasmid pKC8 (*cat araC* $p_{ara}$*::murJ-eGFPΩkan*) was constructed in multiple steps. First, the *kan* cassette was amplified from the pKD4 plasmid using the primers KC273 and KC274. The resulting PCR product was used as a primer for site-directed mutagenesis to introduce the kan marker downstream of the *murJ* gene in the multi-copy suppressor plasmid no. 2 (Supplementary Table 1). A second round of site-directed mutagenesis was performed to fuse *eGFP* in frame with *murJ*. The *eGFP* gene was amplified from the pKC7 plasmid using the primers KC328 and KC329.

Mutant alleles of *murJ* were constructed by site-directed mutagenesis into the plasmid pFLAGMurJΔCys[10] using Phusion high-fidelity DNA polymerase (New England Biolabs) and the primers KC238, KC247, KC248, KC249, KC252, KC253, KC254, KC263 and KC264.

Strains RY34351, RY34352, RY34363, RY34366, RY34376, RY34380 and RY34381 carrying $Lys^M$-resistant mutations were constructed by P1 transduction with $Lys^M$-resistant mutants as donors and RY34350 (*lysA:: frt*, Δ*pyrC::kan*) and plated on M9 minimal medium supplemented with 0.2% (w/v) glucose and lysine (5 μg $ml^{-1}$). The *murJ* loci from transductants were amplified by PCR with the primers KC230 and KC234 and the mutations were confirmed by sequencing. Strain RY34432 was constructed by recombineering the *murJ–e GFPΩkan* PCR fragment, amplified from pKC8 using the primers KC231 and KC234, into the TB28 strain and the resulting recombinants were selected for kanamycin resistance. The *murJ–eGFPΩkan* recombinants were transduced into a clean background

Author Manuscript Author Manuscript Author Manuscript Author Manuscript

(TB28) using P1 transduction. PCR analysis was used to verify the construct at each step of the process.

### Multi-copy suppression

The *E. coli* multi-copy library containing 1–4-kb fragments of chromosomal DNA under $p_{ara}$ control used in this study was constructed for an earlier work[24]. Approximately 200 ng of pooled multi-copy library and ~100 ng of pKC3 plasmid were co-transformed into XL1-Blue by electroporation. The transformants were plated on LB-Ara-Amp-IPTG-X-gal plates to select and screen for survivors. The blue colonies that appeared on the selection plates were picked and the plasmid DNA was extracted using a Qiagen mini-prep kit. The extracted DNA was digested with HindIII and analysed on 0.8% agarose for 1 h at 95 V to separate pKC3 from the multi-copy library plasmid. The slower migrating band was gel-purified using a Qiagen gel-extraction kit, self-ligated, transformed into XL1-Blue, and selected on LB-chloramphenicol (10 μg $ml^{-1}$) plates. The plasmid DNA was extracted with Qiagen mini-prep kit and the junctions were sequenced at Eton Bioscience Inc. with the primers KC30 and KC31. The sequence of the inserts was mapped to the *E. coli* MG1655 genome (NC_000913.3) to identify the possible suppressors. To rule out the suppressors that interfere with arabinose uptake and utilization, the isolates were streaked on M9 minimal agar with arabinose (0.2% w/v) as the sole carbon source.

### Selection and screening for $Lys^M$-resistant mutants

Cultures of XL1-Blue pKC3 were grown to $A_{550\ nm}$~0.2 and *lys*$^M$ was induced with arabinose (0.4% w/v). At ~2 h post-induction, cells were collected from 10 ml of culture through centrifugation at 6,000*g* for 10 min, resuspended in 100 μl LB, and plated on LB-Ara-Amp-IPTG-X-gal plates. The colonies that turned blue after overnight incubation at 37 °C were picked and streak-purified on the same selection media. The $Lys^M$-resistant mutants thus isolated were further characterized in liquid cultures by following their growth post-induction of *lys*$^M$ from pKC3. The expression levels of $Lys^M$–$his_6$ in $Lys^M$-resistant mutants were compared with that in the wild type by western blotting with anti-His (Sigma-Aldrich). The *murJ* locus in $Lys^M$-resistant mutants was amplified by PCR using Phusion high-fidelity DNA polymerase (New England Biolabs) with the primers KC230 and KC234. The amplified PCR product was gel-purified and sequenced with the primers KC230, KC231, KC234 and KC262.

### Microscopy

Strain TB28 pKC3 was grown to $A_{550\ nm}$~0.2 and induced with L-arabinose 0.4% (w/v). At 20 min post-induction, 1 ml of culture was spun down at 14,000*g* for 30 s. The pellet was resuspended in 20 μl, of which 5 μl was spotted on a glass slide with a coverslip on top. Phase-contrast images of the cells were taken with a Zeiss AX10 microscope with × 100 oil immersion objective and 100 ms exposure.

### Plasmid retention assay

TB28 cells carrying plasmids with different mutant alleles of *murJ* were grown to $A_{550\ nm}$~0.2 and induced with 0.4% arabinose. The cell lysates 1 h post-induction were

Author Manuscript Author Manuscript Author Manuscript Author Manuscript

harvested, filter sterilized, and passed through Qiagen DNA binding columns. The bound DNA was eluted with water and transformed into TB28 and the number of transformants was counted. The *murJ* alleles that gave the least number of transformants were scored as tight mutants.

### Detecting lipid II flippase activity with ColM

Lipid II flippase assays were done with slight modifications from previously described[6]. Strain RY34351/pKC4, TU276/pFLAGMurJ/pKC4 and TU276/pFLAGMurJ$^{M233L, I248S}$/pKC4 were grown in LB supplemented with 0.2% (w/v) glucose, 25 μg ml$^{-1}$ of chloramphenicol and 15 μg ml$^{-1}$ ampicillin at 37 °C with shaking overnight. Cultures were then diluted 1:100 into M9 medium supplemented with 0.2% maltose and 100 μg of methionine, lysine and threonine and incubated at 37 °C with shaking. When $A_{600\ nm}$~0.3, 15 μl of [$^3$H]mDAP (1μCi μl$^{-1}$, ARC) was added to 10 ml of culture and arabinose was added to a final concentration of 0.4% (w/v) as indicated. After 15 minutes, 10 μl of colicin M (500 μg ml$^{-1}$) was then added to the culture. Cells were grown for an additional 10 min, immediately chilled on ice, and then harvested by centrifugation at 10,000*g* for 2 min at 4 °C. Spent supernatant was discarded carefully, and cell pellets were resuspended in 1 ml of hot water and further incubated at 100 °C for 30 min. Heat-killed cells (containing labelled lipid intermediates and labelled cell wall) and hot-water extracts (containing soluble labelled PG precursors and ColM product) were separated by centrifugation at 100,000*g* for 20 min at 4 °C. The supernatant fractions containing soluble material were lyophilized, dissolved in 300 μl of buffer A (50 mM triethylammonium formate pH 4.6, 6% (v/v) methanol), followed by HPLC with 70 min isocratic elution of buffer A on a Nucleosil C18 column (Agilent A0119250× 046). Radiolabelled soluble PG precursors and ColM products in the eluate were detected by an inline radioflow detector (Berthold). The hot-water-extracted cell pellets were boiled for 3 min in 1 ml of water to remove residual water-soluble radiolabelled compounds. The washed pellets were then resuspended in 100 μl of 10 mM Tris-HCl pH 7.4. Lipid-linked precursors were extracted from the pellet suspension twice by adding 100 μl of 6 M pyridinium acetate/1-butanol (1:2, v/v) followed by vortexing. The top butanol fractions were carefully transferred to a new tube after centrifugation at 3,000*g* for 30 s and washed once with 100 μl butanol-saturated water. Labelled lipid-linked precursors were then quantified from 100 μl of the butanol fractions (top) by scintillation counting in 10 ml of Ecolite scintillation fluid (882745, MP Biochemicals).

Note that because the radiolabelled soluble compounds were measured using the inline radioflow detector and the lipid intermediates by scintillation counting, the units of radioactivity for quantifying these species are different. Given that the trend of the measurements was clear and consistent (that is, when lipid precursors increased, soluble ColM products decreased and vice versa), we did not think that calibration of the different instruments was necessary.

### Measurement of PG synthesis following ColM treatment

Strain TU276/pFLAGMurJ/pKC4 was grown in LB medium supplemented with 0.2% (w/v) glucose, 25 μg ml$^{-1}$ of chloramphenicol and 15 μg ml$^{-1}$ ampicillin at 37 °C with shaking overnight. Cultures were then diluted 1:100 into 35 ml of M9 medium supplemented with

Author Manuscript Author Manuscript Author Manuscript Author Manuscript

0.2% maltose and 100 μg of methionine, lysine and threonine and incubated at 37 °C with shaking. When cultures reached an $A_{600\ nm}$ of ~ 0.3, 10 ml was transferred to a 50 ml conical tube and 15 μl of [$^3$H]mDAP (1μCi μl$^{-1}$, ARC) was added. Starting at 9 min after label addition, 1 ml samples were withdrawn every 3 min, measured for $A_{600\ nm}$, and transferred to a 1.5 ml tube on ice. Following 15 min of labelling, ColM was added to a final concentration of 500 μg ml to one of the cultures ($t$= 0 in Supplementary Fig. 9). Samples (1 ml) were then withdrawn every 2 min measured for $A_{600\ nm}$, and chilled on ice. Incorporation of label into the PG fraction was performed essentially as previously described[25]. Briefly, samples were centrifuged at 10,000$g$ for 1 min at 4 °C. Cell pellets were resuspended in 1 ml of hot water and further incubated at 100 °C for 30 min to extract labelled soluble PG precursors. Cells were then pelleted by centrifugation at 100,000$g$ for 20 min at 4 °C, washed once with 1 ml of PG buffer (20 mM Tris-HCl pH 7.4, 25 mM NaCl) and resuspended in 0.5 ml of PG buffer. PG was digested by adding 0.25 mg lysozyme and incubated overnight at 37 °C. Insoluble material was pelleted by centrifugation at 20,000$g$ for 20 min at room temperature and radioactivity released into the supernatant fraction by lysozyme (designated labelled PG) was measured by scintillation counting as described above.

## Quantification of the levels of MurJ and Lys$^M$

Cultures (500 ml) of strains RY34159, RY34442 and RY34443 were grown to $A_{550\ nm}$~0.4 units and induced with 0.4% arabinose, the cells were collected 10 min post-induction by centrifugation for 10 min at 10,000 x g (Sorvall Lynx 6000 centrifuge), resuspended in ~4 ml 1× PBS, lysed by passing three times through an Amico French Pressure cell at 16,000 psi, and the cell lysates were cleared of intact cells by centrifugation for 10 min at 10,000$g$ (Sorvall Legend XTR centrifuge). The cleared supernatants (~ 3 ml) were centrifuged at 100,000$g$ (Beckman TL100 centrifuge) to collect membrane fractions, and the membrane fractions were then resuspended in 1 ml of 1× PBS. The membrane fractions from $A_{550\ nm}$~4.0 units, and purified eGFP standards (kindly provided by H. Rye) were mixed with 2× AB buffer (6.84 mM $Na_2HPO_4$, 3.16 mM $NaH_2PO_4$, 50 mM Tris-HCl pH 6.8, 6 M urea, 1% β-mercaptoethanol, 3% SDS, 10% glycerol, 0.1% bromophenol blue) and treated as previously described[10]. The samples were resolved on 4–20% Tris-tricine gel and western blotted with rabbit polyclonal anti-GFP (ab290 from Abcam) at 1:2,000 dilution and goat-anti-rabbit-HRP (ThermoFisher Scientific) at 1:3,000. The protein levels were quantified using ImageJ software.

## Complementation test of pFLAGMurJΔCys derivatives

The ability of pFLAGMurJΔCys-derived plasmids to complement a chromosomal Δ*murJ::frt* allele was tested as previously described[14] using strain NR3267 (NR754 Δ*murJ::frt* pRC7KanMurJ)[9]. Haploid strains carrying complementing pFLAGMurJΔCys-derived plasmids and merodiploid strains NR3942 (NR754 pFLAGMurJΔCys$^{V229G,\ I248S}$) and its wild-type derivative NR2449 (NR754 pFLAGMurJΔCys$^{V229G,\ I248S}$) were processed for western blotting using anti-FLAG M2 (Sigma-Aldrich) and anti-mouse-HRP (GE Amersham). For immunoblots, cells were grown overnight, normalized by $A_{600\ nm}$, pelleted and lysed with 50 μl of SCAM lysis buffer (5 mM Tris-HCl pH 7.4, 1 % SDS, 6 M urea).

Author Manuscript Author Manuscript Author Manuscript Author Manuscript

Prior to loading onto a 10 % SDS–polyacrylamide gel, samples were mixed with 50 μl of 2× AB buffer.

### SCAM

*murJ* haploid strains (Supplementary Table 3) carrying Δ*murJ::frt* pFLAGMurJΔCys derivatives with Cys substitutions at various positions and pKC6 were grown to $A_{600\ nm}$~1.0. Production of $Lys^{M(C10S)}$–myc was induced by the addition of 0.2 % L-arabinose (w/v). After 10 min at 37 °C, cells were pelleted and processed for SCAM as previously described[10].

### $MurJ_{TA}$ structural rendering

The $Lys^{M}$-resistant mutants were rendered on the crystal structure of $MurJ_{TA}$ (PDB 5T77)[11] from *Thermsipho africanus* or the outward-facing model of $MurJ_{TA}$[11] using the UCSF Chimera package[26].

### I-TASSER model of MurJ structure

The *E. coli* MurJ amino-acid sequence (accession no. NP_415587) was submitted to I-TASSER[27]. The model presented here was the model with the highest level of confidence scores (C-score −0.17; TM-score= 0.69±0.12). The top-ranked structural analogue to the model generated by I-TASSER is the recently published structure of the MurJ homologue from *Thermosipho africanus* (PDB 5T77)[11], and comparison of these two structures resulted in a TM-score of 0.894, where 1 indicates a perfect match. Figures were prepared from PBD files downloaded from the I-TASSER server using the PyMOL Molecular Graphics System, Version 1.5.0.4 (Schrödinger, LLC).

### Data availability

The data that support the findings of this study are available from the corresponding authors upon request.

## Supplementary Material

Refer to Web version on PubMed Central for supplementary material.

## Acknowledgments

This work was supported by Public Health Service Grant GM27099 to R.Y., by NIH grant AI099144 and CETR U19 AI109764 to T.G.B., by NIH grant R01GM100951 to N.R., and by the American Heart Association under the award number 14POST18480014 to L.-T.S. Additional support for this work was provided by the Center for Phage Technology at Texas A&M University, jointly sponsored by Texas A&M AgriLife. The authors thank H. Rye and L. Kustigian of the Department of Biochemistry and Biophysics, Texas A&M University, for providing purified eGFP standards.

## References

1. Fischetti VA. Bacteriophage lysins as effective antibacterials. Curr Opin Microbiol. 2008; 11:393–400. [PubMed: 18824123]
2. Bernhardt TG, Wang IN, Struck DK, Young R. Breaking free: “protein antibiotics” and phage lysis. Res Microbiol. 2002; 153:493–501. [PubMed: 12437210]

Author Manuscript Author Manuscript Author Manuscript Author Manuscript


3. Bernhardt TG, Roof WD, Young R. Genetic evidence that the bacteriophage φ X174 lysis protein inhibits cell wall synthesis. Proc Natl Acad Sci USA. 2000; 97:4297–4302. [PubMed: 10760296]
4. Bernhardt TG, Wang IN, Struck DK, Young R. A protein antibiotic in the phage Qβ virion: diversity in lysis targets. Science. 2001; 292:2326–2329. [PubMed: 11423662]
5. Rumnieks J, Tars K. Diversity of pili-specific bacteriophages: genome sequence of IncM plasmid-dependent RNA phage M. BMC Microbiol. 2012; 12:277. [PubMed: 23176223]
6. Sham LT, et al. Bacterial cell wall. MurJ is the flippase of lipid-linked precursors for peptidoglycan biogenesis. Science. 2014; 345:220–222. [PubMed: 25013077]
7. Ruiz N. Bioinformatics identification of MurJ (MviN) as the peptidoglycan lipid II flippase in Escherichia coli. Proc Natl Acad Sci USA. 2008; 105:15553–15557. [PubMed: 18832143]
8. Mohammadi T, et al. Identification of FtsW as a transporter of lipid-linked cell wall precursors across the membrane. EMBO J. 2011; 30:1425–1432. [PubMed: 21386816]
9. Elhenawy W, et al. The O-antigen flippase Wzk can substitute for MurJ in peptidoglycan synthesis in *Helicobacter pylori* and *Escherichia coli*. PLoS One. 2016; 11:e0161587. [PubMed: 27537185]
10. Butler EK, Davis RM, Bari V, Nicholson PA, Ruiz N. Structure-function analysis of MurJ reveals a solvent-exposed cavity containing residues essential for peptidoglycan biogenesis in *Escherichia coli*. J Bacteriol. 2013; 195:4639–4649. [PubMed: 23935042]
11. Kuk AC, Mashalidis EH, Lee SY. Crystal structure of the MOP flippase MurJ in an inward-facing conformation. Nat Struct Mol Biol. 2017; 24:171–176. [PubMed: 28024149]
12. Butler EK, Tan WB, Joseph H, Ruiz N. Charge requirements of lipid II flippase activity in *Escherichia coli*. J Bacteriol. 2014; 196:4111–4119. [PubMed: 25225268]
13. Meeske AJ, et al. MurJ and a novel lipid II flippase are required for cell wall biogenesis in *Bacillus subtilis*. Proc Natl Acad Sci USA. 2015; 112:6437–6442. [PubMed: 25918422]
14. El Ghachi M, et al. Colicin M exerts its bacteriolytic effect via enzymatic degradation of undecaprenyl phosphate-linked peptidoglycan precursors. J Biol Chem. 2006; 281:22761–22772. [PubMed: 16777846]
15. Bernhardt TG, Struck DK, Young R. The lysis protein E of φ X174 is a specific inhibitor of the MraY-catalyzed step in peptidoglycan synthesis. J Biol Chem. 2001; 276:6093–6097. [PubMed: 11078734]
16. Gorzelnik KV, et al. Asymmetric cryo-EM structure of the canonical allolevivirus Qβ reveals a single maturation protein and the genomic ssRNA *in situ*. Proc Natl Acad Sci USA. 2016; 113:11519–11524. [PubMed: 27671640]
17. Krishnamurthy SR, Janowski AB, Zhao G, Barouch D, Wang D. Hyperexpansion of RNA bacteriophage diversity. PLoS Biol. 2016; 14:e1002409. [PubMed: 27010970]
18. Shi M, et al. Redefining the invertebrate RNA virosphere. Nature. 2016; 540:539–543.
19. Osawa S, Furuse K, Watanabe I. Distribution of ribonucleic acid coliphages in animals. Appl Environ Microbiol. 1981; 41:164–168. [PubMed: 7224619]
20. Domingo E, Sabo D, Taniguchi T, Weissmann C. Nucleotide sequence heterogeneity of an RNA phage population. Cell. 1978; 13:735–744. [PubMed: 657273]
21. Domingo E, Holland JJ. RNA virus mutations and fitness for survival. Annu Rev Microbiol. 1997; 51:151–178. [PubMed: 9343347]
22. Baba T, et al. Construction of *Escherichia coli* K-12 in-frame, single-gene knockout mutants: the Keio collection. Mol Syst Biol. 2006; 2:2006.0008.
23. Miller, JH., editor. Experiments in Molecular Genetics. Vol. Ch 28. Cold Spring Harbor Laboratory; Michigan: 1972. p. 201-205.
24. Yunck R, Cho H, Bernhardt TG. Identification of MltG as a potential terminase for peptidoglycan polymerization in bacteria. Mol Microbiol. 2016; 99:700–718. [PubMed: 26507882]
25. Cho H, Uehara T, Bernhardt TG. Beta-lactam antibiotics induce a lethal malfunctioning of the bacterial cell wall synthesis machinery. Cell. 2014; 159:1300–1311. [PubMed: 25480295]
26. Pettersen EF, et al. UCSF Chimera—a visualization system for exploratory research and analysis. J Comput Chem. 2004; 25:1605–1612. [PubMed: 15264254]
27. Roy A, Kucukural A, Zhang Y. I-TASSER: a unified platform for automated protein structure and function prediction. Nat Protoc. 2010; 5:725–738. [PubMed: 20360767]

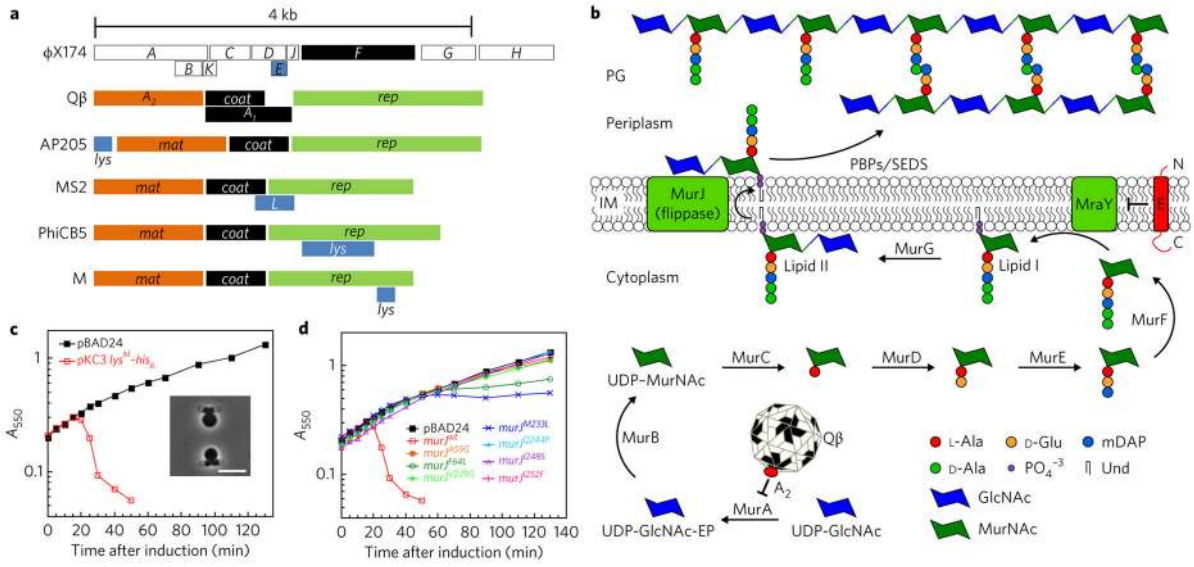


**Fig. 1. The lysis protein of phage M blocks lipid II flipping**

**a**, Genome organization in ssDNA (φ X174) and ssRNA (Qβ, AP205, MS2, PhiCb5, and M) phages. In ssRNA phages, *mat* encodes the maturation protein responsible for adsorption to the receptor pilus, *coat* encodes the capsid protein, and *rep* encodes the replicase. In Qβ, the *mat* gene is named $A_2$ and has the additional function of inducing host lysis. **b**, The PG precursor pathway, from cytoplasmic UDP-GlcNAc to periplasmic lipid II, with known targets of 'protein antibiotics' indicated. **c**, Cells with either pBAD24 (vector) or pKC3 ($lys^M$–$his_6$ clone) were induced with 0.4% (w/v) arabinose and growth was monitored by turbidity. Inset: phase contrast image of cells at 20 min post-induction (scale bar, 5 μm). **d**, Same as **c**, except in hosts producing $Lys^M$-resistant MurJ variants. Throughout, representative lysis profiles from three biological replicates are shown.



Author Manuscript Author Manuscript Author Manuscript Author Manuscript

Author Manuscript Author Manuscript Author Manuscript Author Manuscript

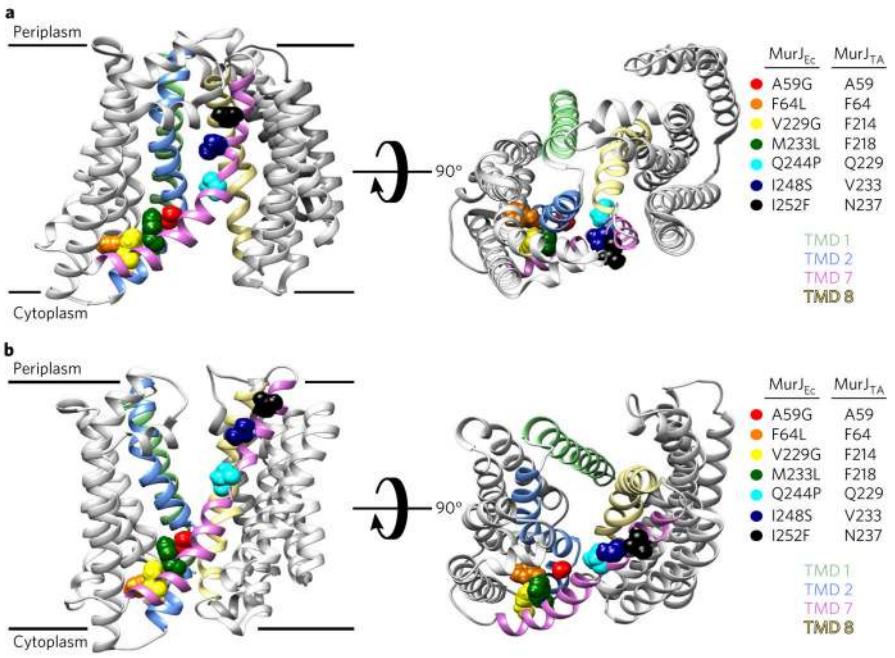


**Fig. 2. Lys$^{M}$-resistance changes map to TMD2 and TMD7 of MurJ**

The amino-acid changes in *E. coli* MurJ ($MurJ_{EC}$) resulting in Lys$^{M}$-resistance were mapped onto the structure of MurJ from *Thermosipho africanus* ($MurJ_{TA}$) (PDB 5T77)[11]. **a**, The cytoplasmic-open conformation. **b**, A model of the periplasmic-open conformation[11]. The TMDs that line the central hydrophilic cavity are coloured: TMD2 (light blue) and TMD7 (magenta). Lateral view (left) and periplasmic view (right). The changes in $MurJ_{EC}$ and homologous amino acids in $MurJ_{TA}$ are shown on the right.

Author Manuscript Author Manuscript Author Manuscript Author Manuscript

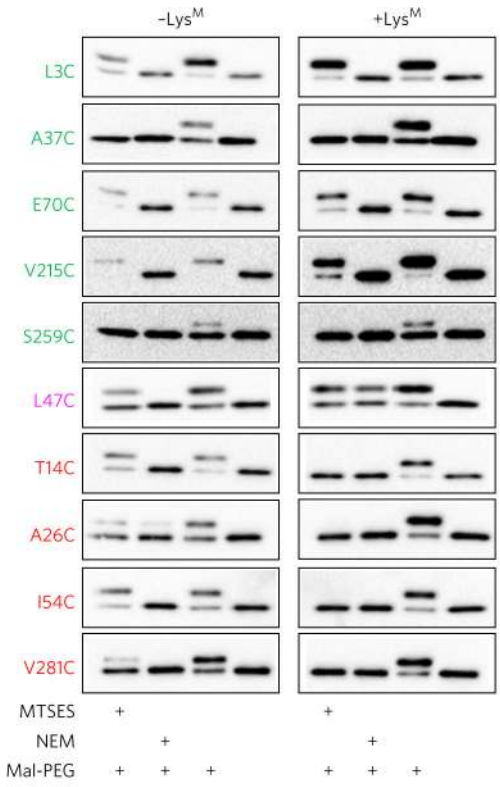


**Fig. 3. Lys$^{M}$ induces conformational changes in MurJ**

The substituted-cysteine accessibility method (SCAM) was used to determine whether the production of Lys$^{M}$ changes the conformation of MurJ in the inner membrane (IM). Conformational changes were reflected as changes in the exposure of cysteine residues introduced at specific positions in MurJ (indicated on the left) to the aqueous periplasm or cytoplasm by comparing SCAM results from samples with or without Lys$^{M}$ production as indicated. Immunoblotting was used to monitor the mass shift in MurJ–FLAG that the thiol-modifying agent Mal-PEG causes unless cysteines were previously modified by IM-permeable NEM (reacts with cysteines exposed to either the periplasm or the cytoplasm) or IM-impermeable MTSES (reacts only with periplasmic cysteines). Substitutions in green showed no change in SCAM pattern; substitutions in pink showed less modification by MTSES and NEM (and therefore more Mal-PEG modification), indicating less exposure to the aqueous environment; and substitutions in red showed more modification by MTSES and NEM (and therefore less Mal-PEG modification), indicating more exposure to the aqueous environment. See Supplementary Fig. 6 for more details. Shown are the representative blots from three biological replicates.

Author Manuscript Author Manuscript Author Manuscript Author Manuscript

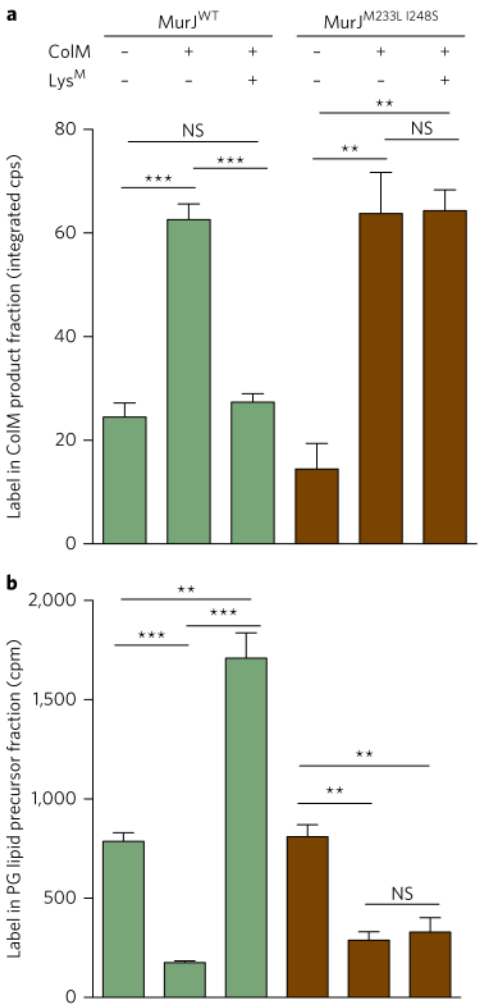


**Fig. 4. Lys$^{M}$ blocks lipid II flipping**

**a**,**b**, Cells of strain TU276 producing FLAG–MurJ$^{WT}$ or FLAG–MurJ$^{M233L, I248S}$ and Lys$^{M}$ from pKC4 as indicated were labelled with [$^{3}$H]mDAP. After 15 min, ColM was added as indicated and growth continued for another 10 min. Samples were then processed to detect label in the soluble ColM product (ColM product) (**a**) and the PG lipid precursor pool (lipid fraction, lipid I and lipid II) (**b**). Shown are the means ± s.e.m. from three experiments. *P* values were determined by Student's *t*-test. Chromatograms of the HPLC results for ColM product quantification are shown in Supplementary Fig. 10. cpm, counts per minute; cps, counts per second. ***$p$< 0.001; **$p$< 0.01; NS, not significant.